

NONLINEAR OPTICAL PHENOMENA

PACS numbers: 42.65.Ky; 42.65.Re; 42.70.Mp
DOI: 10.1070/QE2006v036n01ABEH013102

Phase matching and frequency-noncritical interactions upon frequency conversion of femtosecond pulses

S.G. Grechin, S.S. Grechin

***Abstract*. The phase-matching properties of biaxial nonlinear crystals providing the highly efficient frequency doubling of femtosecond pulses are analysed. The investigation method is based on the separation of the phase-matching condition and frequency-noncritical interaction.**

Keywords: *nonlinear optics, frequency conversion, femtosecond pulses, phase matching, phase-matching bandwidth.*

Femtosecond lasers with frequency conversion are used for solving a variety of problems (see, for example, [1, 2]). The number of active laser media for generating femtosecond pulses and the number of nonlinear crystals for the frequency conversion of femtosecond pulses have continuously increased in the last years. The choice of a nonlinear crystal for frequency conversion is determined by a number of independent requirements. Apart from traditional requirements [a high effective nonlinearity coefficient and the fulfilment of the phase-matching (PM) condition], a large PM spectral width should be also provided for short pulses (with a broad emission spectrum) [3]. The fulfilment of these requirements facilitates the highly efficient conversion of all the spectral components of pulses interacting in a medium, which provides the efficient generation of ultrashort pulses at the sum and difference frequencies. This scope of problems also includes the frequency conversion of tunable lasers and of a broadband radiation (radiation with a great number of non-phased longitudinal laser modes).

The choice of a crystal for frequency conversion of ultrashort pulses is usually based on the minimisation of the group-velocity mismatch of the interacting pulses [2, 4, 5]. It was shown in [6] that this method is a particular case of the method based on the search for the frequency-noncritical phase matching (FNPM)*.

The presence of FNPM in nonlinear crystals can be found qualitatively from the character of the wavelength dependence of the PM direction. In many uniaxial crystals, the wavelength dependence of the PM angle θ has an extremum. Figure 1 shows, for example, such dependences for the two PM types (ooe and oee) upon second harmonic generation (SHG) in a KDP crystal. At the UV boundary of the wavelength range within which PM exists, the PM angle is $\theta = 90^\circ$. As the fundamental radiation wavelength increases, the angel θ decreases. The FNPM regime is realised at the wavelengths for which the PM angle has a minimum (shown by the dashed straight lines in Fig. 1). In this case, the PM direction virtually does not change in a broad wavelength range (the PM condition id fulfilled).

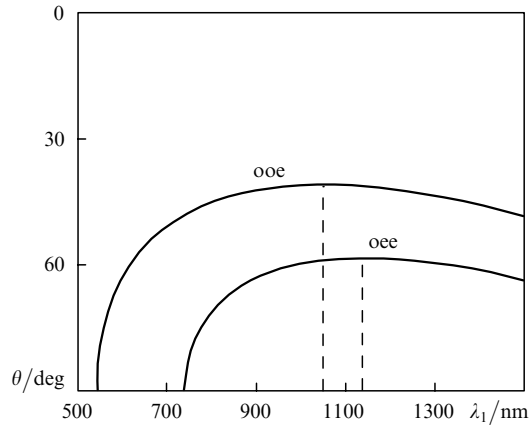

Figure 1. Dispersion of PM directions for a KDP crystal.

While in uniaxial crystals the PM directions form second-order conical surfaces, with the z axis being their bisectrix, in biaxial crystals – these are four-order conical surfaces, and any of the principal axes of the crystal or its optical axes can be their bisectrix. The diagram of PM directions for the SHG in biaxial crystals was first presented in [7]. Later, a more complete diagram was presented [8]. In biaxial crystals, one PM direction distribution passes to another with changing wavelength. Figure 2 shows such transitions for SHG in an LBO crystal. The type of transitions shows that there exists a limiting state which obviously corresponds to the FNPM. For an LBO crystal with the ssf and sff PM, the FNPM is realised in the range from 1200 to 1400 nm. A similar dependence for a KTP crystal is shown in Fig. 3. For this crystal, the FNPM is realised in the range from 1100 to 3700 nm.

* This regime can be also called the wavelength-noncritical phase matching. Below, all the equations will be written for wavelengths because the Sellmeyer equations use the emission wavelength

S.G. Grechin Research Institute of Radio Engineering and Laser Technology, N.E. Bauman Moscow State Technical University, 2-ya Baumanskaya ul. 5, 107005 Moscow, Russia;
e-mail: gera@bmstu.ru;
S.S. Grechin Department of Physics, M.V. Lomonosov Moscow State University, Vorob'evy gory, 119992 Moscow, Russia;
e-mail: grechin@mail.ru

Received 29 September 2005
Kvantovaya Elektronika **36** (1) 45 – 50 (2006)
Translated by M.N. Sapozhnikov

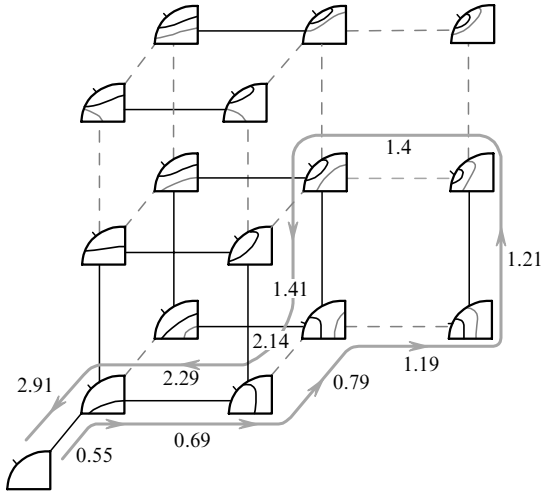

Figure 2. Dispersion of PM directions for an LBO crystal for the ssf (solid lines) and sff (dashed lines) interactions. At the curve with the arrows are indicated the fundamental radiation wavelengths (in μm) at which transitions occur from one distribution to another.

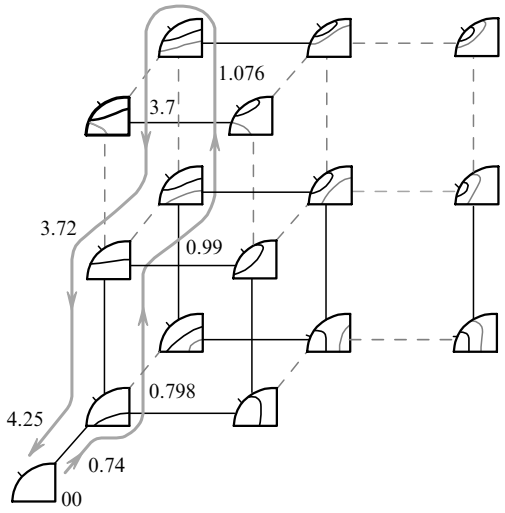

Figure 3. Dispersion of PM directions for a KTP crystal for the ssf (solid lines) and sff (dashed lines) interactions. At the curve with the arrows are indicated the fundamental radiation wavelengths (in μm) at which transitions occur from one distribution to another.

The PM properties of a crystal are commonly used first of all to determine the PM direction. Then, the stability of this direction is considered with respect to variations in external parameters such as the temperature or laser wavelength and also angular deviations from the PM direction. The admissible variation in the parameter is called the PM bandwidth, which is determined from the spectral width $\Delta\lambda$ by using the equation

$$\frac{\Delta k L_{\mathrm{cr}}}{2} = \left[\Delta k_0 + \frac{\partial \Delta k}{\partial \lambda}\,\Delta\lambda + \frac{1}{2}\,\frac{\partial^2 \Delta k}{\partial \lambda^2}\,(\Delta\lambda)^2 + \ldots\right]\frac{L_{\mathrm{cr}}}{2} = \frac{\pi}{2}, \tag{1}$$

where L_{cr} is the crystal length and Δk_0 is the wave detuning for central wavelengths.

To perform the frequency conversion of an ultrashort pulse, a large PM bandwidth is required. The most complete information on the spectral dependence of PM properties $[\Delta k(\varphi, \theta)]$ of a crystal can be obtained by determining, independently of the PM directions, the directions of frequency-noncritical interactions (FNI). These are the directions in which the derivative of the difference of wave numbers $\mathrm{d}\Delta k(\varphi, \theta)/\mathrm{d}\lambda$ is zero. In the general case, the difference of wave numbers in these directions is nonzero $[\Delta k_0(\varphi, \theta) \neq 0]$, but satisfies the condition $\mathrm{d}\Delta k(\varphi, \theta)/\mathrm{d}\lambda = 0$. It is obvious that if the FNI directions exist, they are described by conical surfaces in the space of angles φ and θ, which may not intersect with the PM directions. The FNI directions correspond to the general solution of the frequency conversion problem – the problem of propagation of three waves in a medium (in particular, a linear medium) with the wave vectors changing with the change in the wave frequencies, the difference of the wave vectors being invariable.

The FNI directions can be defined in terms of the difference of the first-order derivatives $[\mathrm{d}\Delta k(\varphi, \theta)/\mathrm{d}\lambda = 0]$ or, for pulses with a broadband spectrum, taking into account higher-order derivatives both for collinear and noncollinear interactions, as

$$\frac{\partial \Delta k(\varphi, \theta)}{\partial \lambda}\,\Delta\lambda + \frac{1}{2}\,\frac{\partial^2 \Delta k(\varphi, \theta)}{\partial \lambda^2}\,(\Delta\lambda)^2 + \ldots = 0. \tag{2}$$

The intersections of the FNI and PM directions correspond to the FNPM directions. In these directions, $\Delta k_0(\varphi, \theta)$ and $\mathrm{d}\Delta k(\varphi, \theta)/\mathrm{d}\lambda$ are zero.

The efficiency of the approach with the independently introduced FNI and PM directions was demonstrated in papers [9, 10] for temperature dependences. This approach was used to determine the wavelength range within which the temperature-noncritical PM was realised. The method of separation of the PM and FNI directions also allows one to analyse simply the possibility of frequency conversion of ultrashort pulses in periodically poled crystals (PPCs) because the structure of these crystals do not change their dispersion properties. In this case, it is reasonable to use the calculation of FNI directions independent of PM. For the FNI directions found in this way, the period of a domain structure at which quasi-PM takes place can be determined.

In this paper, we consider the realisation of FNI and FNPM during SHG in homogeneous crystals. However, this approach can be developed for a more general case of generation of the sum and difference frequencies and parametric generation.

Because the moduli of the wave vectors (or refractive indices) of interacting s and f waves depend on the direction of the wave vector $\boldsymbol{k}$ specified by the angles φ and θ, the derivatives $\partial k(\varphi, \theta)/\partial\lambda$ of these moduli with respect to the wavelength also depend on the direction of the wave vector $\boldsymbol{k}$. In the space of angles φ and θ the FNI directions form conic surfaces, like the PM directions [7, 8]. The difference is in the distributions of directions for the wave vector and its derivative with respect to the wavelength. In the case of a standard (direct) optical arrangement, the refractive indices satisfy the expression $n_z > n_y > n_x$. The normal surfaces for the refractive indices of interacting waves have no discontinuity points but have singularities along the directions of optical axes. Relations between the derivatives $\partial k(\varphi, \theta)/\partial\lambda$ along the principal axes of a crystal are arbitrary. At the

same time, the dependences $\partial k(\varphi,\theta)/\partial\lambda$ for both waves have the discontinuity points in the direction of the optical axis. Similarly to the determination of PM directions [8], we can find the conditions for the existence of the FNI directions in the principal planes of a crystal-optics coordinate system.

One of the primary questions is the question for which of the parameters the FNI directions should be determined: for the difference of wave numbers or the difference refractive indices of the interacting waves. The spatial distributions of these directions will be different. In the FNPM direction, the quantities $\mathrm{d}\Delta k(\varphi,\theta)/\mathrm{d}\lambda$, $\mathrm{d}\Delta n(\varphi,\theta)/\mathrm{d}\lambda$, and $\Delta k(\varphi,\theta)$ are simultaneously equal to zero. Below, we will consider for FNI the expression for the derivative from $\Delta k(\varphi,\theta)$ because it determines the PM bandwidth.

For the ssf interaction in the xy and yz planes, the conditions of the FNI realisation have the form

$$\left[\frac{\mathrm{d}k_z^{(\omega)}}{\mathrm{d}\lambda}-\frac{\mathrm{d}k_y^{(2\omega)}}{\mathrm{d}\lambda}\right]\left[\frac{\mathrm{d}k_z^{(\omega)}}{\mathrm{d}\lambda}-\frac{\mathrm{d}k_x^{(2\omega)}}{\mathrm{d}\lambda}\right]<0 \tag{3}$$

in the xy plane ($\theta=90^\circ$) and

$$\left[\frac{\mathrm{d}k_x^{(2\omega)}}{\mathrm{d}\lambda}-\frac{\mathrm{d}k_z^{(\omega)}}{\mathrm{d}\lambda}\right]\left[\frac{\mathrm{d}k_x^{(2\omega)}}{\mathrm{d}\lambda}-\frac{\mathrm{d}k_y^{(\omega)}}{\mathrm{d}\lambda}\right]<0 \tag{4}$$

in the yz plane ($\varphi=90^\circ$).

The FNI directions in the xz plane differ from PM directions. The wavelength dependence of the angle V_z between the x axis and optical axis can be monotonically increasing or decreasing and can have a minimum or maximum. Figure 4 presents the dependences $V_z(\lambda)$ for some crystals in their transparency ranges. Due to such dependences, the relation of angles between the z axis and optical axes of the fundamental and second-harmonic waves can be arbitrarily [$V_z^{(\omega)}>V_z^{(2\omega)}$, $V_z^{(\omega)}<V_z^{(2\omega)}$ or $V_z^{(\omega)}=V_z^{(2\omega)}$]. Therefore, to determine the FNI directions over the angle θ, we can distinguish three regions: $0<\theta<V_z^{(1)}$, $V_z^{(1)}<\theta<V_z^{(2)}$, and $V_z^{(2)}<\theta<90^\circ$, where $V_z^{(i)}$ are the angles for the fundamental wave ($i=1$) and second harmonic ($i=2$). The conditions of existence of roots for these regions have the form

$$\left[\frac{\partial k_y^{(1)}}{\partial\lambda}-\frac{\partial k_x^{(2)}}{\partial\lambda}\right]\left[\frac{\partial k_y^{(1)}}{\partial\lambda}-\frac{\partial k^{(2)}\left(V_z^{(1)}\right)}{\partial\lambda}\right]<0, \tag{5}$$

$$\left[\frac{\partial k_y^{(1)}}{\partial\lambda}-\frac{\partial k^{(2)}\left(V_z^{(1)}\right)}{\partial\lambda}\right]\left[\frac{\partial k^{(1)}\left(V_z^{(2)}\right)}{\partial\lambda}-\frac{\partial k_y^{(2)}}{\partial\lambda}\right]<0, \tag{6}$$

$$\left[\frac{\partial k^{(1)}\left(V_z^{(2)}\right)}{\partial\lambda}-\frac{\partial k_y^{(2)}}{\partial\lambda}\right]\left[\frac{\partial k_z^{(1)}}{\partial\lambda}-\frac{\partial k_y^{(2)}}{\partial\lambda}\right]<0. \tag{7}$$

For the sff interaction in the xy and yz planes, the conditions of FNI realisation can be obtained by replacing $k_{x,y}^{(2\omega)}$ by $\frac{1}{2}(k_{x,y}^{(2\omega)}+k_z^{(2\omega)})$ in (3) and replacing $k_{z,y}^{(\omega)}$ by $\frac{1}{2}(k_{z,y}^{(\omega)}+k_x^{(\omega)})$ in (4). For the xz plane, the conditions have the form

$$\left[\frac{1}{2}\left(\frac{\partial k_x^{(1)}}{\partial\lambda}+\frac{\partial k_y^{(1)}}{\partial\lambda}\right)-\frac{\partial k_x^{(2)}}{\partial\lambda}\right]\left[\frac{\partial k_y^{(1)}}{\partial\lambda}-\frac{\partial k^{(2)}\left(V_z^{(1)}\right)}{\partial\lambda}\right]<0, \tag{8}$$

$$\left[\frac{\partial k_y^{(1)}}{\partial\lambda}-\frac{\partial k^{(2)}\left(V_z^{(1)}\right)}{\partial\lambda}\right]\times\left\{\frac{1}{2}\left[\frac{\partial k_y^{(1)}}{\partial\lambda}+\frac{\partial k^{(1)}\left(V_z^{(2)}\right)}{\partial\lambda}\right]-\frac{\partial k_y^{(2)}}{\partial\lambda}\right\}<0, \tag{9}$$

$$\left\{\frac{1}{2}\left[\frac{\partial k_y^{(1)}}{\partial\lambda}+\frac{\partial k^{(1)}\left(V_z^{(2)}\right)}{\partial\lambda}\right]-\frac{\partial k_y^{(2)}}{\partial\lambda}\right\}\times\left[\frac{1}{2}\left(\frac{\partial k_z^{(1)}}{\partial\lambda}+\frac{\partial k_y^{(1)}}{\partial\lambda}\right)-\frac{\partial k_y^{(2)}}{\partial\lambda}\right]<0. \tag{10}$$

The conditions of FNI existence for all possible types of interaction (sss, fss, ffs, etc.) realised in PPCs can be determined similarly.

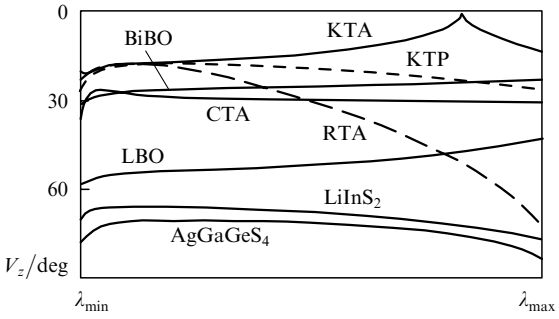

Figure 4. Dispersion of the angle V_z between the z axis and the optical axis for different crystals.

The PM directions never coincide with the optical axis direction (see, for example, [10]), which follows from the relation for the principal values of the refractive index and the presence of dispersion. The FNI directions can be located both around optical axes, corresponding to the waves with different frequencies, and between the axes. Figure 5 shows the first derivative of wave-number difference with respect to the detuning wavelength in the xz plane as a function of the angle θ for the sss interaction in a KTP crystal at a wavelength of 2400 nm. One of the zeroes of this dependence is located between $V_z^{(1)}$ and $V_z^{(2)}$. The second zero takes place in the optical axis direction [the angle $V_z^{(1)}$]. Similar dependences can be realised for all possible types of interaction.

By generalising the results presented above, we obtained the FNI directivity diagram (Fig. 6). In the general case, the FNI directions can be absent. They can appear along any of the principal axes of a crystal. The distribution of FNI

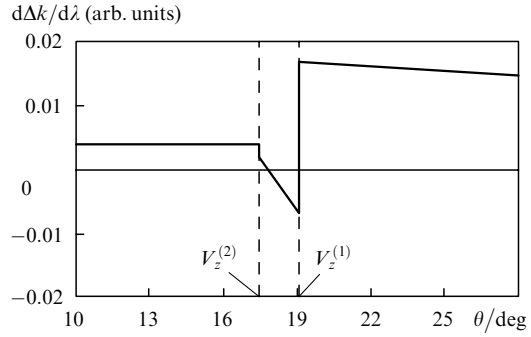

Figure 5. Derivative of the difference of wave numbers with respect to the wavelength as a function of the angle θ.

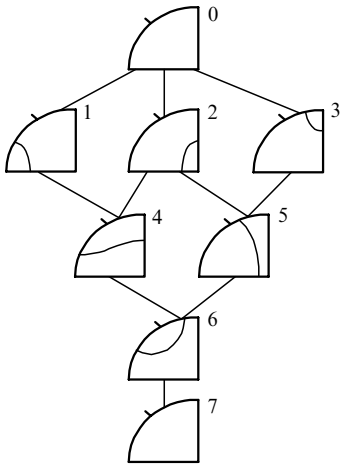

Figure 6. FNI directivity diagram.

directions over the lines connecting diagrams changes with changing the wavelength.

Consider the realisation of these directions by the example of an LBO crystal. Figures 7 and 8 show the distributions of the FNI and PM directions for the ssf and sff interactions for different fundamental radiation wavelengths. For the ssf interaction and the fundamental radiation wavelength $\lambda < 554$ nm, the FNI and PM directions are absent. For $\lambda = 554$ nm, PM along the y axis appears. As the wavelength increases, the cone of PM directions expands. For $\lambda = 687.1$ nm, the PM direction passes from the yz to xz plane. Then, the PM direction cone 'contracts' to the x axis. For $\lambda = 875.7$ nm, the FNI along the y axis appears. At this stage, variations in the FNI direction for an LBO crystal are similar to variations in the PM direction. The PM and FNI direction cones intersect in the xz plane for $\lambda = 1260$ nm along a straight line located

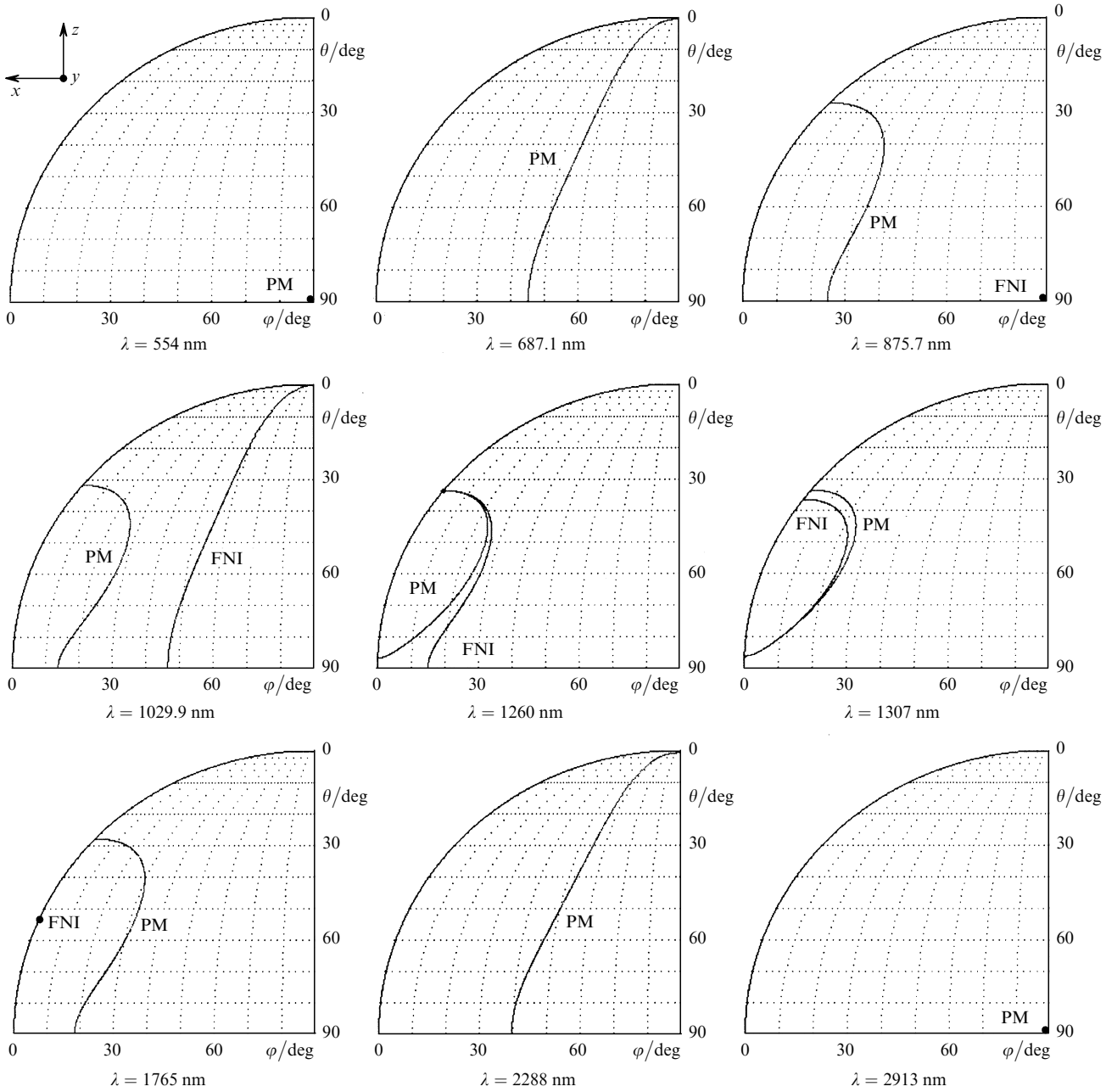

Figure 7. FNI and PM directivity diagrams for the ssf interaction in an LBO crystal.

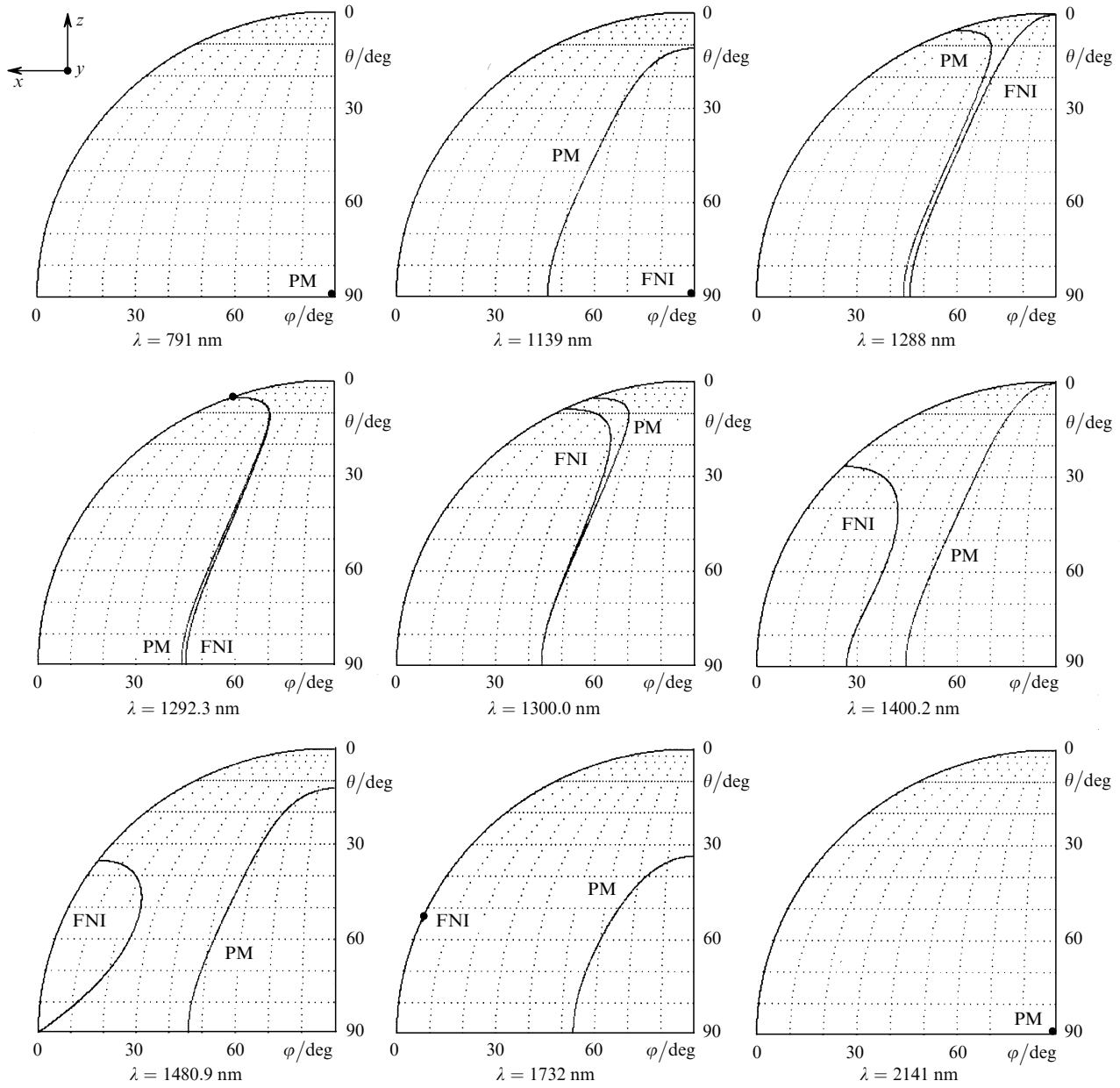

Figure 8. FNI and PM directivity diagrams for the sff interaction in an LBO crystal.

above the optical axis. The efficient nonlinearity coefficient in this region is identically zero.

As the wavelength is further increased, the rate of variation in the FNI directions becomes greater than that in the PM directions, resulting in the displacement of the intersection point of the conic surfaces in the diagram (Fig. 7). For $\lambda = 1307$ nm, as in the first case, the intersection occurs in the xz plane, but below the optical axis. In this region, the effective nonlinearity coefficient is maximal. As the wavelength is further increased, the FNI directions 'contract' to the optical axis and the FNI disappears for $\lambda =$ 1765 nm. The PM direction cone changes by 'contracting' to the y axis. For $\lambda = 2913$ nm, PM disappears.

Therefore, for the ssf interaction in an LBO crystal, PM exists in the wavelength range 554 – 2913 nm, the FNI in the range 875.7 – 1765 nm, and the FNPM in the range 260 – 1307 nm. The most preferable is the FNPM in the xy plane (at $\lambda = 1307$ nm), where the effective nonlinearity coefficient has the maximum value. As the wavelength is decreased, the FNPM is realised not in the principal planes of the crystal, and the effective nonlinearity coefficient monotonically decreases to zero.

Variations in the PM and FNI directions in the case of the sff interaction in an LBO crystal are similar (Fig. 8). PM exists in the wavelength range 791 – 2141 nm, the FNI in the range 1139-1732 nm, and the FNPM in the range 1292.3 – 1300 nm. For this type of interaction, the effective nonlinearity coefficient is maximal along the z axis. For both types of interaction in an LBO crystal, the $0-2-5-6-7$ transitions occur in the FNI directivity diagram (Fig. 6).

Analysis of the FNI realisation conditions (3) – (10) shows that during SHG, a solitary FNI directivity cone can exist in the space of angles φ and θ. In a more general case of three-frequency interaction (sum and difference frequency generation), when the frequencies of all interacting waves are different, variations in the FNI direction are

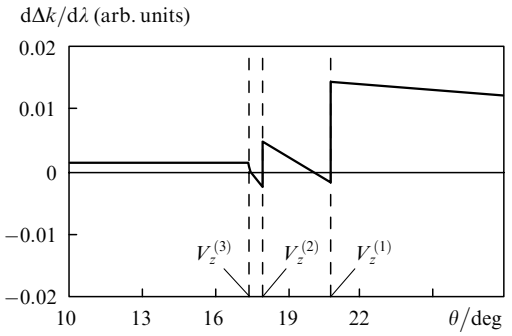

Figure 9. Derivative of the difference of wave numbers with respect to the wavelength as a function of the angle θ for the sss interaction ($\lambda_1 = 3100$ nm, $\lambda_2 = 1815$ nm).

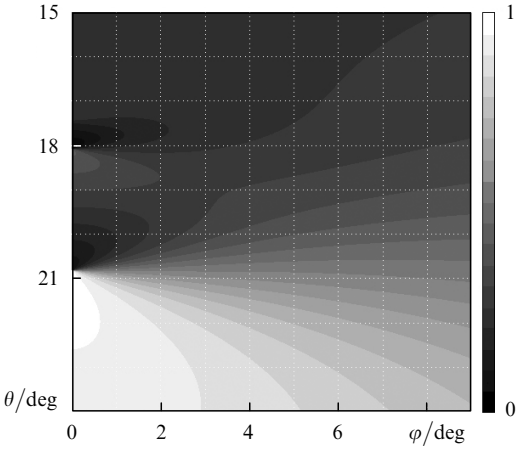

Figure 10. Derivative of the difference of wave numbers with respect to the wavelength as a function of the angles θ and φ for the sss interaction ($\lambda_1 = 3100$ nm, $\lambda_2 = 1840$ nm). The brightness gradation with a step of 0.05.

similar as a whole to variations in these directions of the second harmonic. A special feature is that more that two roots can be obtained in the xz plane. This is explained by the fact that the derivatives $\partial\Delta k(\varphi,\theta)/\partial\lambda$ have the discontinuity along the optical axes of the crystal. Figure 9 shows the dependence of the derivative of the difference of wave numbers with respect to the wavelength on the angle θ in the xz plane for the sss interaction. Figure 10 presents the distribution of the derivative $\partial\Delta k(\varphi,\theta)/\partial\lambda$ as a function of the angles φ and θ in the vicinity of optical axes. In this region for a fixed value of the angle φ, four values of the angle θ exist at which $\partial\Delta k(\varphi,\theta)/\partial\lambda = 0$.

Finally, we can make the following conclusions. The separation of the PM and FNI directions can be efficiently used to analyse the possibility of frequency conversion of ultrashort pulses. The FNI directions form conic surfaces, which are similar to those appearing upon PM. As the fundamental radiation wavelength is changed, the FNI directions change. The rate and character of variations in the FNI and PM directions are different. The directions in which the FNI and PM directivity cones intersect are the FNPM directions. In biaxial crystals, these directions take place in a certain wavelength range. Thus, the FNPM regime is realised in an LBO crystal in the wavelength ranges from 1260 to 1307 nm (the ssf interaction) and from 1292.3 to 1300 nm (the sff interaction).

References

1. Cerullo G., De Silvestri S. *Rev. Sc. Instr.*, **74**, 1 (2003).
2. Petrov V., Rotermund F., Noack F. *J. Opt. A: Pure Appl. Opt.*, **3**, R1 (2001).
3. Dmitriev V.G., Tarasov L.V. *Prikladnaya nelineinaya optika* (Applied Nonlinear Optics) (Moscow: Fizmatlit, 2004).
4. Xia J., Wei Z., Zhang J. *Opt. Laser Technol.*, **32**, 241 (2000).
5. Dubietis A., Tamosauskas G., Varanavicius A. *Opt. Commun.*, **186**, 211 (2000).
6. Grechin S.S., Pryalkin V.I. *Kvantovaya Elektron.*, **33**, 737 (2003) [*Quantum Electron.*, **33**, 737 (2003)].
7. Hobden M.V. *J. Appl. Phys.*, **38**, 4365 (1967).
8. Grechin S.G., Grechin S.S., Dmitriev V.G. *Kvantovaya Elektron.*, **30**, 377 (2000) [*Quantum Electron.*, **30**, 377 (2000)].
9. Grechin S.G., Dmitriev V.G., D'yakov V.A., Pryalkin V.I. *Kvantovaya Elektron.*, **34**, 461 (2004) [*Quantum Electron.*, **34**, 461 (2004)].
10. Grechin S.G., Dmitriev V.G., D'yakov V.A., Pryalkin V.I. *Izv. Ross. Akad. Nauk. Ser. Fiz.*, **66**, 4365 (2002).